AIAA 81-0308R

Cloud Encounter and Particle Number Density Variabilities from GASP Data

G. D. Nastrom*
Control Data Corporation, Minneapolis, Minn.
J. D. Holdeman†
NASA Lewis Research Center, Cleveland, Ohio
and
R. E. Davis‡
NASA Langley Research Center, Hampton, Va.

Summary statistics and variability studies are presented for cloud encounter and particle number density data taken as part of the NASA Global Atmospheric Sampling Program (GASP) aboard commercial Boeing 747 airliners. On average, cloud encounter is shown on about 15% of the 52,164 data samples available, but this value varies with season, latitude, synoptic weather situation, and distance from the tropopause. The number density of particles (diameter greater than 3 μm) also varies with time and location, and depends on the horizontal extent of cloudiness.

Introduction

THE purpose of this paper is to present the first results from a new and unique data set of cloud encounter and particle number density measurements near the tropopause. While the extent and density of clouds are of daily concern to nearly everyone, clouds and their composition are of importance in a professional sense primarily to meteorologists and aviators. To the meteorologist clouds are, of course, the primary physical manifestation of storm systems in the troposphere and are direct harbingers of surface weather events.[1] But clouds also play an important role in less widely appreciated facets of meteorology. For example, the vertical air currents in clouds transport large amounts of heat and horizontal momentum through the atmosphere, thus influencing the development of large-scale storm systems. Also, the extent and density of cirrus clouds are major factors in the Earth's radiation balance,[2] and may influence the long-period (climate) variations of global temperature.[3,4]

Early aviators avoided clouds because they did not have instrument navigation aids and could easily become lost or disoriented in clouds. More recently, certain clouds have been avoided because of potential hazardous turbulence or possible aircraft icing.

Clouds are also of interest for proposed laminar flow control (LFC) wing aircraft. This interest, which provided the motivation for this study, is due to some evidence that the low drag characteristics of LFC wings are lost (albeit temporarily) whenever visible clouds are encountered, and are lost occasionally as well in cirrus hazes,[5,6] thereby influencing the economic feasibility of LFC.

The data in this study were collected as part of the NASA Global Atmospheric Sampling Program (GASP)[7,8] described below. Interested readers can find complete statistical summaries and tabulations of the cloud and particle data in Ref. 9. The present paper presents only a sample of the results to illustrate the major features of variability in space and time. It is believed that this is the first presentation of in situ cloud encounter measurements near the tropopause on a global basis.

Presented as Paper 81-0308 at the AIAA 19th Aerospace Sciences Meeting, St. Louis, Mo., Jan. 12-15, 1981; submitted March 4, 1981; revision received July 20, 1981. This paper is declared a work of the U.S. Government and therefore is in the public domain.

*Meteorologist.
†Aerospace Engineer. Member AIAA.
‡Meteorologist.

Data

The cloud encounter and particle concentration data used in this study cover the period from December 1975 through December 1977. These data are from GASP tapes VL0004-VL0014 which have been archived at the National Climatic Center, Asheville, N.C., and which are described elsewhere.[10]

The data acquisition phase of GASP, which ended in June 1979, obtained meteorological and trace constituent data with instruments placed aboard as many as four Boeing 747 airliners in routine commercial service. Data were recorded at nominal 5 or 10 min intervals during flight above about 6 km (20 kft). In addition to the basic GASP measurements, the tropopause pressure at each GASP data location has been time and space interpolated from the National Meteorological Center (NMC) grids when available and added to the archival tapes. Auxiliary meteorological data used here, such as vorticity, have been computed for each GASP data location from the NMC isobaric height fields.[11] Other details concerning the GASP measurements and instrumentation are given in Refs. 8 and 12 and references therein.

The presence of clouds at cruise altitude was determined with a light-scattering particle counter.[13] This aspect of the GASP cloud and particle instrumentation is described further in Ref. 9. A cloud detection threshold level was set, based on visual observation of a light haze outside the aircraft. The same threshold level was used for all GASP instruments and resulted in an "in-cloud" registration whenever the local particle number density (for particle diameter >3 μm) was greater than 66,000/m^3. The sampling time for the cloud detector was 256 s, or approximately 66 km (41 statute miles) at a 500 knot ground speed. At the end of each sampling cycle for the GASP system, the number of seconds (out of the preceding 256) which registered as "in cloud" was recorded.

During the first minute of each sampling period, the number of particles in each of three size ranges was counted. The size ranges were D (diam) >0.45, 1.4, and 3 μm. Although GASP cloud data were first reported in December 1975,[13] particle count data were not reported until January 1977 due to a rather large uncertainty in the total particle count resulting from nonuniform illumination of the sample chamber and high noise-to-signal ratio on channels measuring particles of less than 1.4 μm diam.[14] Only the channel

counting of the largest particles ($D > 3$ μm), designated PD5 in the GASP data reports, has been used here because only the largest particles are believed to contribute to the LFC loss.

Before proceeding, it is necessary to establish some nomenclature which will be used repeatedly in the analyses to follow. First, it is convenient to separate GASP observations according to whether the indicated time in clouds during the observation period was equal to, or greater than, zero. The total indicated time-in-clouds divided by the total observation time gives the fraction of the time-in-clouds, denoted TIC. Those observations with TIC = 0 are termed *in-clear*, and those with TIC > 0 (but not necessarily equal to 100%) are interpreted to be in the vicinity of clouds and are denoted CIV. The time-in-clouds divided by the total observation time for only those observations with TIC > 0 gives the fraction of time in clouds in the vicinity of clouds, denoted TICIV. All of these quantities are expressed as percentages in the analyses.

Results

During the period December 1975 through December 1977, 960 GASP flights reported cloud detection data. There are 52,164 individual cloud encounter observations in all. As shown in Fig. 1, these data are most numerous in Northern Hemisphere midlatitudes but are fairly evenly distributed by season. The hatched areas in Fig. 1 show observations in the vicinity of clouds (CIV), that is, those with TIC > 0. The numbers above the bars indicate percentage CIV in each interval. Of the total 52,164 data points, 7,647 (14.7%) are in or in-the-vicinity of clouds.

The distribution of cloud encounter observations as a function of distance from the NMC tropopause is given in Fig. 1c. Because NMC tropopause data were occasionally not available, there are only 48,214 observations here. This panel clearly illustrates that very few clouds are encountered in the stratosphere. In fact, the frequency of clouds in the stratosphere may be even less than indicated because the tropopause pressures are interpolated from large-scale grids (2.5° latitude by 2.5° longitude × 12 h), while the GASP data are local measurements and small-scale undulations of the tropopause may be missed by the NMC grid.

Cloud encounter data are used here as reported, with all observations given equal weight, although it must be pointed out that not all observations are independent. Because general cloudiness (or the lack thereof) is not a random event but is associated with large-scale weather systems, clear and cloudy areas tend to have appreciable areal extent. For example, the data in Table 1 indicate there is an 83.5% random chance that any observation will be cloud-free, but that if the previous observation was also cloud-free, this probability increases to 95%. Similarly, there is only a 16.5% random chance that any observation will be in the vicinity of clouds (TIC > 0), compared to a 75% chance if the previous observation was in the vicinity of clouds, and 79% chance if the previous two observations were in the vicinity of clouds. The persistence in Table 1, or lack of independence among consecutive observations, can be verified subjectively by recalling that both clear and cloudy areas often have a large spatial extent as seen, say, from a satellite picture or from a ground observer's perspective.

Table 1 Persistence of cloud encounter data

	Probability that present observation will be		
	Clear	TIC > 0	TIC > 10%
Random	83.5	16.5	12.2
If previous observation was:			
Clear	95.0	5.0	2.5
TIC > 0	24.9	75.1	61.6
TIC > 10%	17.5	82.5	72.9
If previous two observations were:			
Clear	96.0	4.0	1.9
TIC > 0	21.0	79.0	66.0
TIC > 10%	14.8	85.2	74.7

The distribution of cloud encounter data with respect to the distance from the NMC tropopause is further illustrated by the cumulative frequency distributions in Fig. 2. These curves give the percentage of observations (on the ordinate) in which the TIC equaled or exceeded any given percentage TIC (on the abscissa). The upper curves, which pertain only to observations with TIC > 0 and labeled CIV, show no significant variability with respect to the distance below the tropopause.

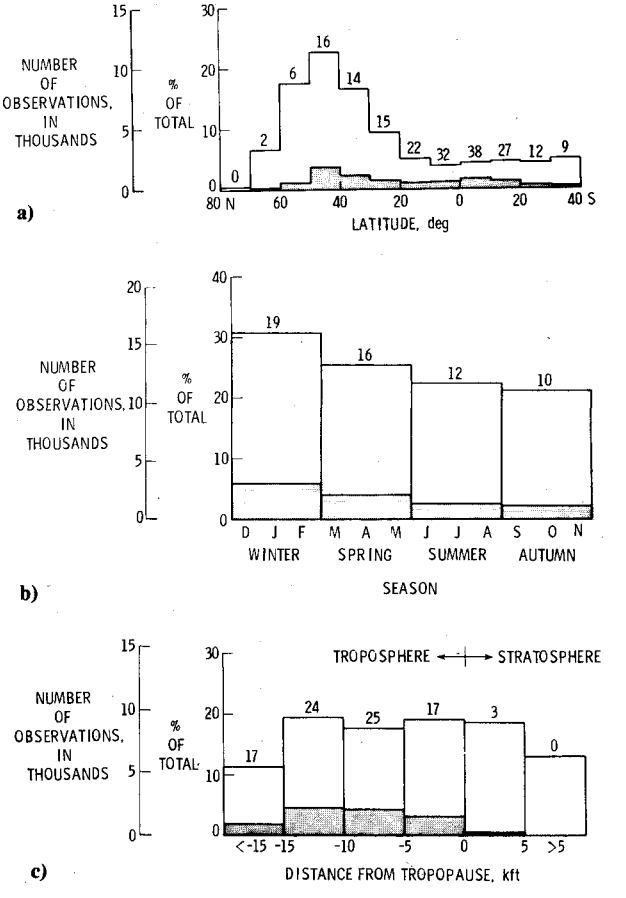

Fig. 1 a) Distribution of cloud detection observations by latitude. b) Distribution of cloud detection observations by season. c) Distribution of cloud detection observations by distance from NMC tropopause.

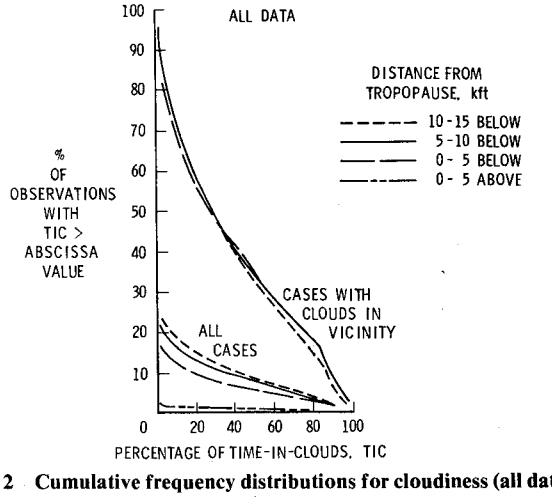

Fig. 2 Cumulative frequency distributions for cloudiness (all data).

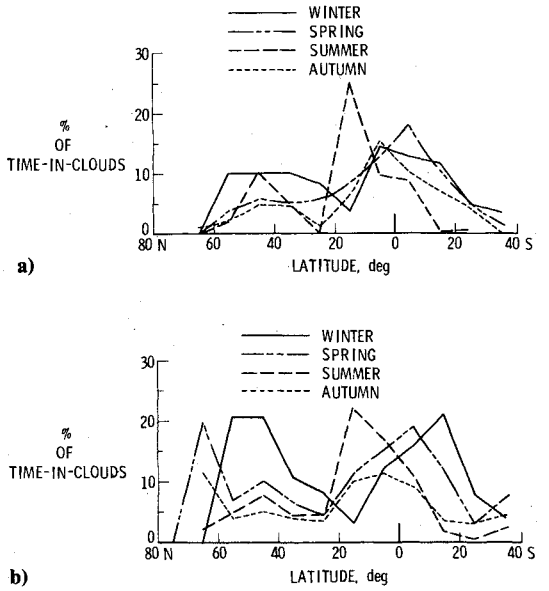

Fig. 3 a) Variation of time-in-clouds by latitude and season, 33.5-38.5 kft altitude region; b) Variation of time-in-clouds by latitude and season, all tropospheric data.

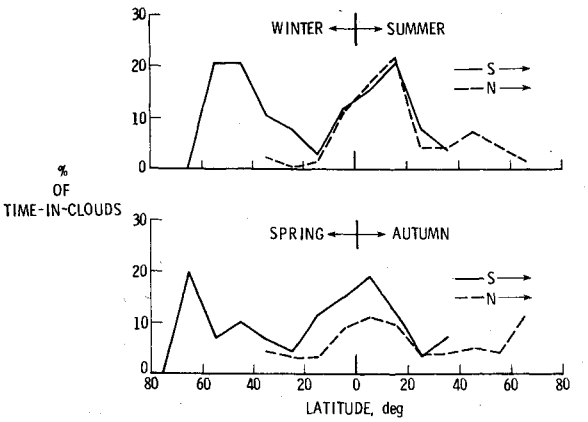

Fig. 4 Seasonal symmetry of percentage time-in-clouds with latitude.

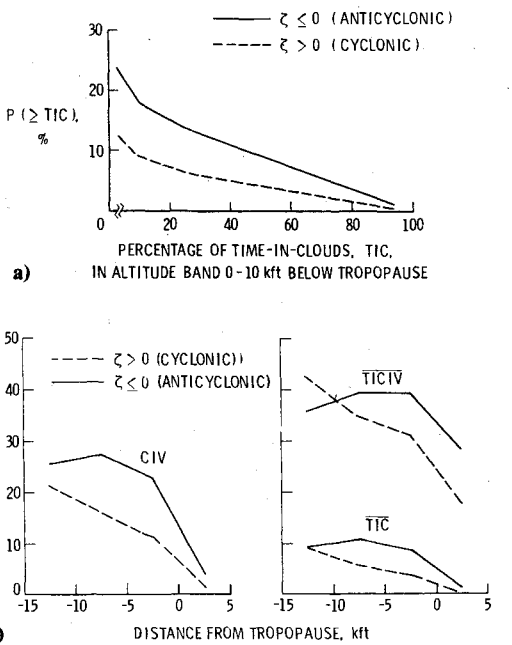

Fig. 5 a) Cumulative frequency distributions of cloudiness with relative vorticity ζ; b) Variation in cloudiness parameters with distance from tropopause.

The median value of TIC for the upper curves is near 28% in all cases. The lower curves for all data show that the probability of encountering any given percentage TIC decreases slightly as the tropopause is approached from below, with a large discontinuity apparent at the tropopause.

Variations with latitude and season of the percentage of TIC for the pressure altitude range of 33.5-38.5 kft (10.2-11.8 km) are presented in Fig. 3a, and for all tropospheric data in Fig. 3b. Some of the variability, especially at high latitudes, in Fig. 3a can be explained by seasonal variations of the mean height of the tropopause. For example, the small TIC during winter at 65°N is largely because these are nearly all stratospheric data (cf., Fig. 1c). This clearly illustrates that great care must be used when interpreting results based on mixed tropospheric and stratospheric data. Thus, further discussion will be confined to the tropospheric-only data in Fig. 3b.

Many features in Fig. 3b may be related to the global-scale circulations. The general latitudinal march of maxima and minima in cloudiness at low latitude is explained by the seasonal migration of the Intertropical Convergence Zone (ITCZ). This region of maximum cloudiness ranges between approximately 18°N in summer and 18°S in winter. The Hadley cells existing to the north and south of the ITCZ shift northward and southward along with it, resulting for the Northern Hemisphere in maximum descending motions (minimum cloudiness) near 35°N in summer and 15°N in winter. Thus, in Fig. 3b, during winter the depressed values of cloud encounter frequency in the 10-20°N interval and enhanced values south of 10°N are consistent with the zonal mean Hadley circulation which has its axis near 10°N with descending motions to the north and ascending motions to the south of the axis.[15] The following additional specific features of Fig. 3b are noted and appear consistent with the global circulation:

1) The peak in mean cloudiness generally seems to occur near the subsolar latitude (sun overhead at noon), lagging it by a few degrees. In winter the peak occurs near 15°S, in spring at 5°S, in summer at 15°N, and for autumn at 5°N. The interhemispheric symmetry in comparable seasons is striking (see also Fig. 4) but not unexpected.

2) A local maximum near 45°N is noted in all the curves in Figs. 3b and 4. This is believed to be the result of the increased frequency of cyclone encounter along the Northern Hemisphere polar front. The effect is largest in winter as would be expected, because the maximum intensity of the midlatitude baroclinic storm systems is achieved then. Indeed, for the winter season, the secondary and primary maxima are of equal magnitude. Due to the lack of airline routes at high latitudes in the Southern Hemisphere, no comparable relative maximum can be verified at this time, but one might be expected on symmetry considerations.

3) The value of the principal maximum seems to be fairly invariant for winter, spring, and summer at 18-22% probability of cloud encounter; for autumn, a figure of 12% is obtained.

4) A latitudinal displacement of the minimum of cloud encounter also occurs during the year, with the minimum point's latitude preceding the poleward or equatorward march of the subsolar point. In winter, this feature is farthest south, lying near 15°N. In spring the point moves to 25°N, in summer it reaches 35°N, and then retreats to 25°N again in autumn. For the Southern Hemisphere the data, although limited in latitudinal extent, suggest a relative minimum near 35°S in winter (Southern Hemisphere summer) and a flat minimum region near 25°S for the other seasons. The minima for each hemisphere and seasonal combination occur near a value of 1-3%.

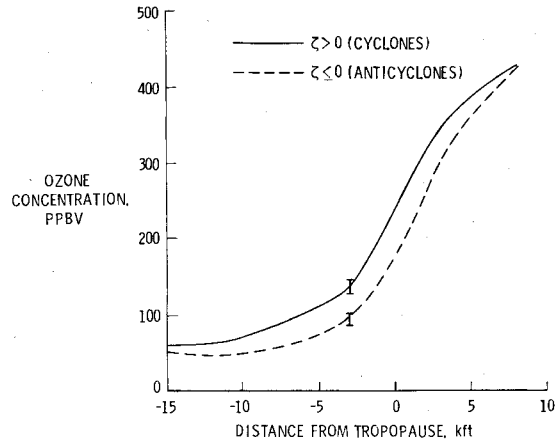

Fig. 6 Variation of ozone with distance from tropopause in cyclones and anticyclones.

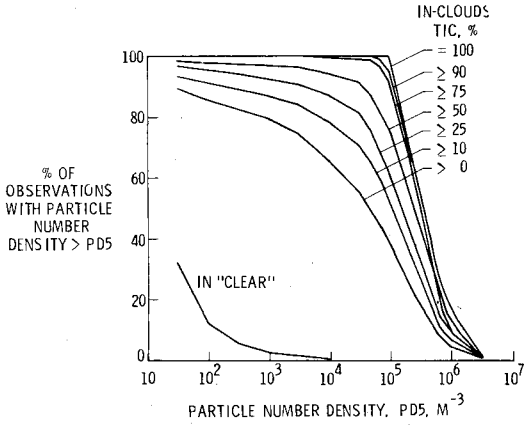

Fig. 7 Cumulative frequency distributions for particles ≥3 μm in diameter.

As noted earlier in connection with the persistence of cloudiness, cloudiness is related to large-scale storm systems (a general model can be found in Ref. 16). An objective variable for separating the two fundamental dynamic regimes, cyclones and anticyclones, is the relative vorticity.[16] Figure 5a shows the cumulative frequency distribution for all data separated only by the algebraic sign of the vorticity (a cyclone's flow has positive vorticity, an anticyclone's negative). Note that this difference is slightly larger than the difference between layers below the tropopause (cf., Fig. 2). The differences between cyclonic and anticyclonic conditions with respect to distance from the tropopause (Fig. 5b) are striking and are consistent with the ozone distributions in cyclones and anticyclones given in Fig. 6. The latter results confirm those obtained earlier by another method.[17] In fact, for the present data in the troposphere, the observed ozone levels are consistently and significantly lower for observations with CIV than for those in clear air.[9] While other factors may have an influence on ozone (e.g., photochemistry, dissociation at the surface of ice crystals), it seems most likely that this result is a consequence of the well-known tendency for ozone levels in the upper troposphere to be relatively low in anticyclones and high in cyclones.

As stated earlier, GASP cloud encounter data began in December 1975 but particle density data (PD5) did not begin until January 1977. A first concern with the PD5 data was therefore to establish the degree to which statistics of this subset resemble statistics of the entire cloud encounter data set. For this purpose, counterparts of Figs. 1 and 2 were constructed (not shown here, see Ref. 9), except that only records for which PD5 data were available were used. The main features of variability in the new figures were not different from Figs. 1 and 2, and therefore it was concluded that the PD5 data subset is representative.

It is, of course, expected that particle densities will be different in clear and cloudy air. Figure 7 shows the cumulative frequency distribution (cfd) of all available PD5 data separated by the associated TICs. Among observations in the vicinity of clouds, the probability of encountering any given particle density increases as the percentage TIC increases. (This result might have been expected because, if PD5 is very small in clear air and very large in dense clouds, then as TIC increases larger average PD5 values should be obtained.) Note, however, that the differences among the CIV curves are small compared with the difference between clear and "cloudy" air shown by the TIC = 0 and >0 curves.

It is of interest to note the particle number densities in totally cloudy air (TIC = 100%) and in clear air (TIC = 0). As explained in Ref. 9, these values are of special interest for the LFC impact problem, but they should also be of interest for meteorological purposes. In clear air the global annual mean of PD5 is less than 100 m^{-3}.§ In cloudy air, only 12 observations have TIC = 100%, so the following statistical model of PD5, based on the observation (see Fig. 7) that as TIC increases the median value of PD5 also increases, was postulated to estimate PD5 (TIC = 100%). In fact, the regression model

$$\log \mathrm{PD5} = a + b(\mathrm{TIC}/100)$$

using all data with TIC > 0 accounts for about one-third of the variance of log PD5 on a global and annual basis. The model was also constructed for subsets of the data as functions of latitude, season, altitude, and distance from the NMC tropopause. For these subsets the percentage of explained variance ranged from about 20% to nearly 50%, but standard statistical tests showed that the regression coefficients a and b determined for each subset were not different (at the 95% confidence level) from the values found using all data. The global annual model has $a = 2.96$ and $b = 3.09$, which give

$$\mathrm{PD5\ (TIC = 100\%)} = (1.12 \pm 0.28) \times 10^6 \mathrm{m}^{-3}$$

$$\mathrm{PD5\ (TIC = 0)} = (912 \pm 155)\ \mathrm{m}^{-3}$$

where the 95% level has been used for the statistical error estimates. This estimate of PD5 (TIC = 100%) is four times larger than that obtained from the 12 available measurements (2.95×10^5 m^{-3}), and suggests that both values should be verified when more data become available.

The rationale for applying the cloud encounter and particle number density statistics gleaned from the GASP data to the estimation of laminar flow (LF) loss is given in Ref. 9 and will not be delineated fully here. However, some examples of the results obtained, using conservative assumptions, will be given below to indicate the utility of the GASP data for the estimation of LF loss.

Application to LFC Studies

It was established in Ref. 9 that flight in clear air should result in no loss of LF. Also, based on Hall's LF loss criterion,[6] the GASP cloud encounter results show that more than 10% LF loss would always be experienced within clouds. Thus, flight within clouds would always result in a significant loss of LF. For simplicity and conservativism it is assumed that all encounters with clouds always cause a total (but

§As explained in Ref. 14, the minimum detectable particle count is 30 m^{-3}, and values less than 30 are recorded as zero. Of the 17,580 observations made in clear air, 11,855 had PD5 = 0 and the mean value of the other 5725 observations was 238 m^{-3}. If we assume that all PD5 values recorded as zero are really PD5 = 15, then the average PD5 in clear air is 88 m^{-3}.

Table 2 Preliminary cloud encounter statistics over three routes in summer and winter

Code: No. of observations
P(TIC>0%), % P(TIC≥10%), %
P(TIC>25%), % P(TIC≥50%), %

Altitude band, kft / Route	Summer						Winter					
	28.5 - 33.5		33.5 - 38.5		38.5 - 43.5		28.5 - 33.5		33.5 - 38.5		38.5 - 43.5	
JFK-LHR	No data		17 0 0	0 0	262 0.8 0.8	0.8 0.8	50 20.0 6.0	16.0 2.0	89 31.5 25.8	27.0 22.5	12 0 0	0 0
JFK-LAX	4 25.0 0	25.0 0	14 50.0 7.1	21.4 0	17 5.9 0	5.9 0	72 34.7 25.0	29.2 18.1	277 23.1 17.0	19.1 12.3	262 0.8 0.4	0.4 0.4
LAX-HNL	7 0 0	0 0	29 0 0	0 0	41 0 0	0 0	259 20.8 12.7	17.0 9.3	869 20.4 10.9	15.5 6.8	320 3.8 1.6	2.8 0.9

Table 3 Preliminary cloud encounter statistics on Los Angeles to Tokyo route in summer and winter

Code: No. of observations
P(TIC>0%), % P(TIC≥10%), %
P(TIC≥25%), % P(TIC≥50%), %

Route segment (approx) and lat/long cell used in simulation	Altitude band, kft: Summer						Winter					
	28.5 - 33.5		33.5 - 38.5		38.5 - 43.5		28.5 - 33.5		33.5 - 38.5		38.5 - 43.5	
1) LAX-35°N/120°W 30-40° N/75-120°W	4 25.0 0	25.0 0	14 50.0 7.1	21.4 0	17 5.9 0	5.9 0	72 34.7 25.0	29.2 18.1	277 23.1 17.0	19.1 12.3	262 0.8 0.4	0.4 0.4
2) 35°N/120°W-40°N/125°W 30-40 °N/120-165°W	30 23.3 6.7	16.7 6.7	120 9.2 4.2	5.0 1.7	173 6.4 1.2	3.5 0	267 22.8 12.0	17.6 8.2	682 21.3 13.8	16.6 10.3	351 4.6 1.7	2.0 0.9
3) 40°N/125°W-50°N/145°W 40-50°N/120-165°W	7 14.3 0	0 0	206 33.5 15.5	22.8 5.8	317 14.2 4.4	8.2 1.3	16 37.5 12.4	25.0 6.3	63 25.4 17.6	20.6 4.8	29 3.4 0	0 0
4) 50°N/145°W-55°N/165°W 50-60°N/120-165°W	No data		113 18.6 5.3	8.8 0.8	143 0 0	0 0	14 0 0	0 0	43 0 0	0 0	42 0 0	0 0
5) 55°N/165°W-50°N/165°E 50-60°N/165°W-150°E	No data		111 9.9 0.9	4.5 0	366 2.5 0.5	1.1 0	No data		39 0 0	0 0	85 0 0	0 0
6) 50°N/165°E-40°N/150°E 40-50°N/165°W-150°E	No data		352 38.6 18.8	26.7 12.2	384 9.6 3.9	6.0 1.8	No data		33 0 0	0 0	40 0 0	0 0
7) Composite of cells 3-6 35°N/120°W-40°N/150°E 40-60°N/120°W-150°E	Insuff. data		782 30.3 13.4	19.9 7.2	1210 7.5 2.6	4.4 0.9	Insuff. data		178 9.0 6.2	7.3 1.7	196 0.5 0	0 0
8) 40°N/150°E-HND 30-40°N/150-105°E	28 28.6 25.0	25.0 17.9	117 40.2 23.1	29.9 15.4	103 15.5 3.9	8.7 2.9	13 0 0	0 0	20 0 0	0 0	18 0 0	0 0

temporary) loss of LF. Then the estimate of the fraction of time that LF loss occurs along a given route is assumed equal to the fraction of time-in-cloud along the route.

Tables 2 and 3, adapted from Ref. 9, are presented as examples of cloud encounter statistics over specific routes, as derived from a subset of the GASP data. First, in Table 2, TIC statistics for the routes New York to London (JFK-LHR), New York to Los Angeles (JFK-LAX), and Los Angeles to Honolulu (LAX-HNL) are given for summer and winter and for the three altitude bands 28.5-33.5, 33.5-38.5, and 38.5-43.5 kft above mean sea level. Within each block, the number of observations making up the sample, the probability of cloud encounter P(TIC≥0%), the probability of being in clouds at least 10% of the time P(TIC≥10%), 25% P(TIC≥25%), and 50% P(TIC≥50%) of the time are given. As an example of using the data in the table, consider the cloud encounter probabilities on the New York to Los Angeles route. In the winter one would expect to encounter clouds (and, by our assumption, lose LF) 34.7% of the time, when flying in the 28.5-33.5 kft altitude band. By flying in the

33.5-38.5 kft band, the cloud encounter probability could be reduced to around 23%; in the 38.5-43.5 kft band, there is less than 1% probability of cloud encounter. For the same route in the summer, it is noted that the probability of cloud encounter is generally greater, as might be expected from the greater probability of convective cloud development over land in summer. It is noted, however, that several of the sample sizes are small and the statistical uncertainty is large, so one must use caution in comparing the data from different altitude bands and different seasons in these cases.

Table 3 presents statistics obtained over a longer route, Los Angeles to Tokyo, where, in the analysis of the GASP data, the cloud cover is described in terms of statistics for each of several contiguous latitude-longitude cells along the route. Again, caution must be employed when cell sample sizes are small but, just as for Table 2, the expected improvement with increasing altitude exists in general. It is shown in Ref. 9 that the probability of cloud encounter generally decreases with increasing altitude worldwide, and that in all cases the uppermost altitude band (38.5-43.5 kft) shows the highest promise for cloud avoidance.

It should be emphasized here that the present results are based on only the data from December 1975 to December 1977. In the next phase of our research, the remainder of the GASP data, extending through June 1979, will be included in the analysis; this will result in larger sample sizes and greater confidence.

Conclusions

1) About 15% of all observations indicate some cloudiness (TIC > 0). If only data in the troposphere are considered, then about 22% indicate some cloudiness.

2) For those observations indicating some cloudiness (TIC > 0), the median time in cloud is about 28%.

3) The seasonal and latitudinal variations of the mean time in cloud show close correspondence with salient features of the general circulation. In particular, the equatorial symmetry at low latitudes during corresponding seasons is remarkably high.

4) Less cloudiness (and higher ozone) is measured in cyclones than in anticyclones, in agreement with classical models of synoptic circulation systems.

5) The mean particle number density in clear air (for $D > 3$ μm) is less than 100 m^{-3}, while the value in dense clouds is 1.12×10^6 m^{-3}. The latter estimate is from a regression model and should be verified as more observations become available.

6) The statistical data derived for cloud encounter are suitable for estimating the probability of flight within cloud (and laminar flow degradation) along airline routes. As expected, the probability of cloud encounter generally decreases with increase in cruise altitude.

References

[1] Brooks, C. F., "The Use of Clouds in Forecasting," *Compendium of Meteorology,* edited by T. F. Malone, American Meteorological Society, Boston, 1951, pp. 1167-1178.

[2] Platt, C. M. R., "Remote Sounding of High Clouds, I: Calculation of Visible and Infrared Optical Properties from Lidar and Radiometer Measurements," *Journal of Applied Meteorology,* Vol. 18, Sept. 1979, pp. 1130-1143.

[3] Schneider, S. H., "Cloudiness as a Global Climate Feedback Mechanism: The Effects on the Radiation Balance and Surface Temperature of Variations on Cloudiness," *Journal of Atmospheric Sciences,* Vol. 29, Nov. 1972, pp. 1413-1422.

[4] Cess, R. D., "Climate Change: An Appraisal of Atmospheric Feedback Mechanisms Employing Zonal Climatology," *Journal of the Atmospheric Sciences,* Vol. 33, Oct. 1976, pp. 1831-1843.

[5] Braslow, A. L. and Muraca, R. J., "A Perspective of Laminar-Flow Control," AIAA Paper 78-1528, Aug. 1978.

[6] Hall, G. R., "On the Mechanics of Transition Produced by Particles Passing Through an Initially Laminar Boundary Layer and the Estimated Effect on the LFC Performance of the X-21 Aircraft," Northrop Corp., Hawthorne, Calif., Oct. 1964.

[7] Perkins, P. J. and Gustafsson, U. R. C., "An Automated Atmospheric Sampling System Operating on 747 Airliners," NASA TMX-71790, 1975.

[8] Perkins, P. J. and Papathakos, L. C., "Global Sensing of Gaseous and Aerosol Trace Species Using Automated Instrumentation on 747 Airliners," NASA TM-73810, 1977.

[9] Nastrom, G. D., Holdeman, J. D., and Davis, R. E., "Cloud Encounter and Particle Concentration Variabilities from GASP Data," NASA TP-1886, Dec. 1981.

[10] Briehl, D., Dudzinski, T. J., and Liu, D. C., "NASA Global Atmospheric Sampling Program (GASP): Data Report for Tape VL0014," NASA TM-81579, 1980.

[11] Nastrom, G. D., "Variability and Transport of Ozone at the Tropopause from the First Year of GASP Data," NASA CR-135176, 1977.

[12] Gauntner, D. J. et al., "Description and Review of Global Measurements of Atmospheric Species from GASP," NASA TM-73781, 1977.

[13] Holdeman, J. D., Humenik, F. M., and Lezberg, E. A., "NASA Global Atmospheric Sampling Program (GASP): Data Report for Tape VL 0004," NASA TM X-73574, 1976.

[14] Holdeman, J. D. et al., "NASA Global Atmospheric Sampling Program (GASP): Data Report for Tapes VL 0010 and 0012," NASA TM-79061, 1979.

[15] Newell, R. E. et al., "The General Circulation of the Tropical Atmosphere and Interactions with Extratropical Latitudes, Vol. I," Massachusetts Institute of Technology, Boston, 1972.

[16] Palmen, E. and Newton, C. W., *Atmospheric Circulation Systems,* Academic Press, New York, 1969.

[17] Holdeman, J. D., Nastrom, G. D., and Falconer, P. D., "An Analysis of the First Two Years of GASP Data," NASA TM-73817, 1977.